Formulation of an alternative analytical solution technique for magnetostatic field problems (repository copy)

Article:

Chama, A, Gerber, S., Wang, R-J., (2017) Formulation of an alternative analytical solution technique for magnetostatic field problems, *Proc. of the 25th Southern African Universities Power Engineering Conference*, (SAUPEC), pp. 305--308, Stellenbosch, 30 Jan. - 1 Feb. 2017.

FORMULATION OF AN ALTERNATIVE ANALYTICAL SOLUTION TECHNIQUE FOR MAGNETOSTATIC FIELD PROBLEMS

A Chama*, S Gerber* and R-J Wang*

* *Department of Electrical and Electronic Engineering, Stellenbosch University, Private Bag X1, Matieland 7602, South Africa. E-mail: chama@aims.ac.za, sgerber@sun.ac.za, rwang@sun.ac.za*

Abstract: Analytical magnetic field calculations are often used in the electrical machine design and analysis. Since the solutions presented are generally in form of Fourier series without error estimation, the numeric convergence and accuracy are not always guaranteed. In many cases higher number of harmonic terms are required to obtain a satisfactory result and in some situations the solution may still become divergent. In this paper an alternative analytical solution technique is proposed, which shows both good convergence performance and accuracy. To validate the proposed solution technique some examples are considered and the results compared with the finite element method.

Key words: Analytical field solution, Fourier series, Fourier transform, Magnetic fields.

1. INTRODUCTION

Magnetic field analysis has been widely used in the design and analysis of electromagnetic devices such as electrical machines, transformers, actuators, magnetic gears and couplers, etc. [1–3]. For accurate field solution different methods can be used to numerically or analytically solve the governing Maxwell equations. The most popular numerical method is the finite element method (FEM), which is known to give accurate results. However, FEM calculation is computationally expensive, especially when it is incorporated in a design optimization [4, 5]. For such situation analytical methods are sometimes preferred alternatives [6].

There is numerous work on the exact solution of the vector potential formulation of magneto-static problems [1, 6], in which the solutions presented are in form of Fourier series without error estimation. In many cases higher number of harmonic terms are required to obtain a satisfactory result [7] and in some situations the solution may experience convergence issues [8]. For the sake of clarity, let's consider for instance the magnetization vector function **M** shown in Figure 1.

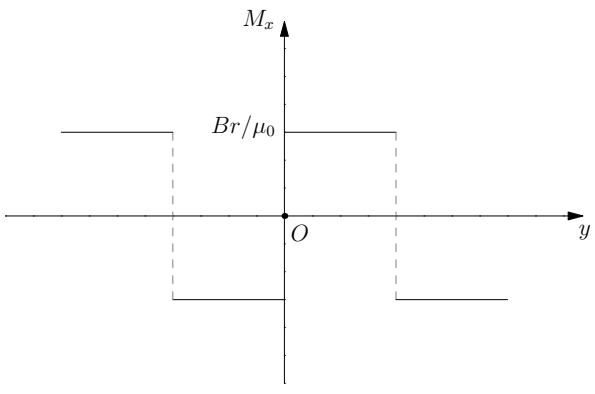

(a)

Figure 1: Magnetization vector

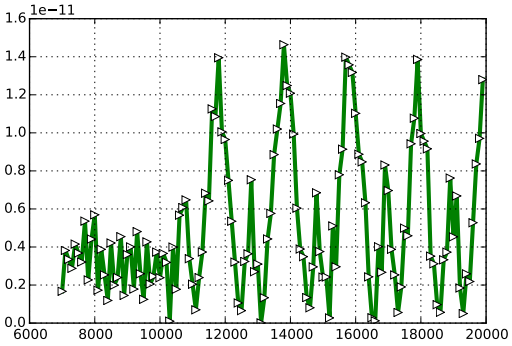

Figure 2: Residual of the curl of the magnetic field approximation using Fourier series

Using Fourier series, **M** can be expressed as

$$\nabla \times \mathbf{M} = \sum_n \frac{2B_r}{L}[\cos(n\pi) - 1]\cos(\frac{n\pi}{L}y) \qquad (1)$$

where L and B_r are half of the periodicity and the intensity of **M**, respectively.

Figure 2 shows an instability of the residual and nothing guarantees its convergence to zero. Clearly, the general term $u_n = [\cos(n\pi) - 1]\cos(\frac{n\pi}{L}y)$ in (1) does not converge to zero when $n \to \infty$ and hence the series is divergent.

In this paper a new analytical solution technique that could provide better convergence performance is proposed. The rest of this paper is organized as follows. In Section 2 the solution domain and the formulation of its vector potential problem are described. In Sections 3 and 4 the resolution of the problem and the error estimate are presented. The numerical implementation of the proposed technique is given in Section 5. Relevant conclusions are drawn in Section 6.

2. VECTOR POTENTIAL PROBLEM FORMULATION

Consider a bounded domain Ω subset of $\mathbb{R}^d$, that constitute a magnetic device, with Lipschitz boundary Γ. The vector potential formulation of Maxwell equations is:

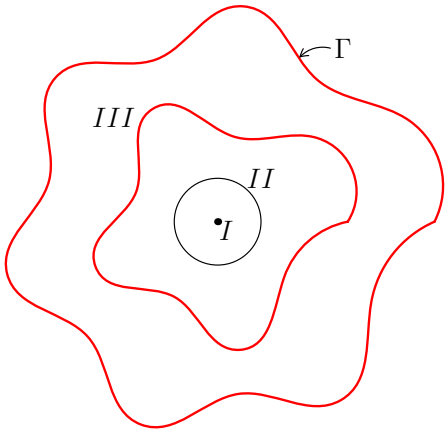

(a)

Figure 3: Domain Ω

(I) In the air-gaps

$$-\frac{1}{\mu}\nabla^2\mathbf{A} = 0; \tag{2a}$$

(II) In the magnet regions

$$-\frac{1}{\mu}\nabla^2\mathbf{A} = \frac{1}{\mu}\nabla\times\mathbf{M}; \tag{2b}$$

(III) In the steel

$$-\frac{1}{\mu}\nabla^2\mathbf{A} = 0; \tag{2c}$$

where μ is the permeability of the medium and $\mu = \mu_0$ in the air-gap region, $\mu = \mu_0\mu_m$ in the magnet region and $\mu = \mu_0\mu_r$ in the steel region, μ_m and μ_r are relative permeability, $\mathbf{M}$ is the magnetization vector and $\mathbf{A}$ is the vector potential which constitutes the unknown variable to be determined. Dirichlet boundary condition $\mathbf{A} = 0$, is imposed on Γ.

3. ANALYTICAL SOLUTION METHOD

In this section the analytical technique for solving problem (2) is described in detail.

The standard analytical approach is to treat (2) independently, each with its own sub-domain and boundary conditions. This renders the method complex and cumbersome and produces in general a slow convergent Fourier series. An alternative way is to consider the system in (2) as a single differential equation, such that:

$$\nabla^2\mathbf{A} = F(X), \tag{3}$$

where X is a physical variable that defines the position inside the domain and $F(X)$ is an implicit function of the magnetization vector (e.g. $\nabla\times\mathbf{M}$) or $\mathbf{J}$ if X is inside the magnet or current regions and zeros else. $F(X)$ also depend on the permeability of the materials.

For situation where permanent magnets are used in region II, it is given by

$$F(X) = \begin{cases} \mu(X)\,\nabla\times\mathbf{M} & \text{for } X\in\Omega_{II} \\ 0 & \text{for } X\in\Omega_I\cup\Omega_{III}\,, \end{cases} \tag{4a}$$

In the case that current density is applied to regions I and II, (4) can be written as

$$F(X) = \begin{cases} \mu(X)\,\mathbf{J} & \text{for } X\in\Omega_I \\ -\mu(X)\,\mathbf{J} & \text{for } X\in\Omega_{II} \\ 0 & \text{for } X\in\Omega_{III}\,, \end{cases} \tag{4b}$$

where Ω_I, Ω_{II} and Ω_{III} are the sub-domains shown in Figure 3 and $\mu(X)$ is permeability function. In all cases $\mu(X)$ is defined such that the following continuity condition across the boundaries of the regions is satisfied

$$\frac{1}{\mu_I}\nabla\times A_I = \frac{1}{\mu_{II}}\nabla\times A_{II}$$

For example, in the first part of (4a) $\mu(X)$ takes the value one inside region II (magnets) and $\mu = \dfrac{\mu_I\cdot\mu_{II}}{\mu_I+\mu_{II}}$ at the boundary with region I.

For simplicity and because in general the magnetization vector $\mathbf{M}$ is unidirectional, as indicated in Figure 1, it is assumed that $\mathbf{A}$ depends on a single physical variable. Now consider $\widetilde{A}$ and $\widetilde{F}$ to be the Fourier transform of A and F, which means that:

$$A(x) = \frac{1}{2\pi}\int_{-\infty}^{\infty}\widetilde{A}(\omega)e^{i\omega x}\mathrm{d}\omega \tag{5a}$$

$$F(x) = \frac{1}{2\pi}\int_{-\infty}^{\infty}\widetilde{F}(\omega)e^{i\omega x}\mathrm{d}\omega \tag{5b}$$

From Equations (5a) and (3) we have

$$\frac{1}{2\pi}\int_{-\infty}^{\infty}\omega^2\widetilde{A}(\omega)e^{i\omega x}\mathrm{d}\omega = \frac{1}{2\pi}\int_{-\infty}^{\infty}\widetilde{F}(\omega)e^{i\omega x}\mathrm{d}\omega, \tag{6}$$

which implies that

$$\widetilde{A}(\omega) = \frac{1}{\omega^2}\widetilde{F}(\omega) \;\text{ and }\; A(x) = \int_{-\infty}^{\infty}\frac{1}{w^2}\widetilde{F}(\omega)e^{i\omega x}\mathrm{d}\omega \tag{7a}$$

Using the properties of $\mathbf{M}$ as shown in Figure 1, see also [6], (7a) can be transformed into

$$A(x) = 2\int_0^{\infty}\frac{1}{\omega^2}\widetilde{F}(\omega)\sin(\omega x)\mathrm{d}\omega. \tag{7b}$$

If we define the boundary Γ to be $x = L$ then

$$A(L) = 0 \;\rightarrow\; \sin(\omega L) = 0 \;\rightarrow\; \omega = \frac{n\pi}{L},\;\forall n\in\mathbb{N}. \tag{7c}$$

Note that the function $\frac{1}{\omega}\sin(\omega x)$ for $\omega = 0$ is the derivative of $\sin(\omega x)$ at $\omega = 0$, which is $\omega\cos(\omega x)|_{\omega=0} = 0$. Combining (7b) and (7c), it follows that

$$A(x) = \frac{2\pi}{L}\sum_{n=1}^{\infty}\frac{1}{\omega_n^2}\widetilde{F}(\omega_n)\sin(\omega_n x), \tag{8}$$

where we have used the fact that $\frac{1}{w}\sin(\omega x)|_{\omega=0} = 0$, $\omega_n = \frac{n\pi}{L}$ and $d\omega = \Delta\omega_n = \omega_{n+1} - \omega_n = \frac{\pi}{L}$.

From (2a) and (2b) one can observe the value of μ can be simplified except for the boundaries of the sub-domains where the value μ is defined by using the permeabilities of two different regions.

4. ERROR ANALYSIS

For (8) to converge to its exact solution the residual R_N, given by

$$R_N = \sum_{n=N}^{\infty} A_n = \frac{2\pi}{L}\sum_{n=N}^{\infty}\frac{1}{\omega_n^2}\widetilde{F}(\omega_n)\sin(\omega_n x) \tag{9}$$

must converge to zeros when $N \to \infty$, where N is the number of harmonics and A_n are the terms of the series A. To establish that $\lim_{N\to\infty} R_N = 0$, we observe that

$$\begin{aligned} |R_N| &\le \frac{2\pi}{L}\sum_{n=N}^{\infty}|\frac{1}{\omega_n^2}\widetilde{F}(\omega_n)\sin(\omega_n x)| \\ &\le \frac{1}{2\pi L}\sum_{n=N}^{\infty}\frac{1}{n^2} \le C_0\int_N^{\infty}\frac{1}{x^2}\mathrm{d}x = C_0\frac{1}{N} \end{aligned} \tag{10}$$

which clearly shows that the residual R_N tends to zero as $N \to \infty$.

5. NUMERICAL IMPLEMENTATIONS

To validate the developed solution technique two case studies are given in this section. In the first case F is a function of the magnetization vector whereas in the second case F is a function of current density.

5.1 Case I

In this example the magnetization vector **M**, that defines the functional F in (2b) is depicted in Figure 1 with $B_r = 1.05$ and $\mu_0 = 4\pi\times10^{-7}$. The domain in consideration is shown in Figure 4(a), with $\mu_r = 1000$ and $\mu_m = 1.05$. The exact solution of (8) in this context is given by:

$$A(y) = \sum_{n=1}^{\infty}\frac{4b}{(n\pi)^2}\sin(\frac{n\pi}{b}a)\sin(\frac{n\pi}{b}y) \tag{11}$$

Figure 4(b) shows the good agreement between the results obtained using the proposed solution technique and the finite element method.

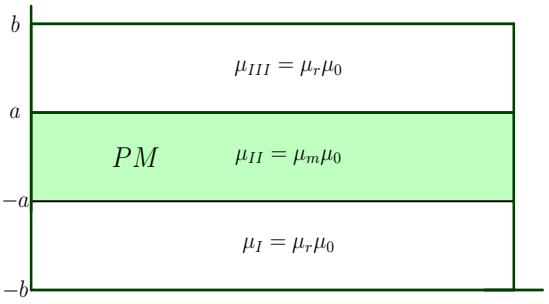

(a)

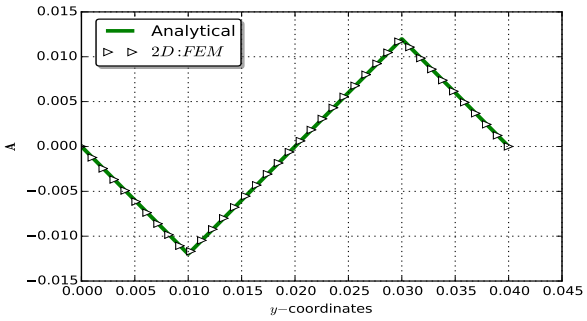

(b)

Figure 4: (a) Material properties; (b) Graphical representations: FEM and Analytical

5.2 Case II

The domain of consideration in this example is similar to the one in 5.1, with the exception that the current density is used instead, see Figure 5(a). One can use similar approach to find the solution of (2b). However, due to the nature of **J** the transformation of $J = \nabla\times X$ is used, in order to obtain similar expression to (3), and also divide the domain into current and steel regions.

Solution: Using the Fourier transform of $\nabla\times X$ in the current and steel regions we have

$$\begin{aligned} A(x) = &\frac{4J_0\mu_0}{b}\sum_{n=1}^{\infty}\frac{1}{\omega_n^3}\sin(W\omega_n)\sin(\omega_n C)\sin(\omega_n x) \\ &+\frac{2\mu}{b}\sum_{n=1}^{\infty}\frac{1}{\omega_n^2}\sin(a\omega_n)\sin(\omega_n x) \end{aligned} \tag{12}$$

where $W = \frac{b-a}{2}$, $C = \frac{b+a}{2}$ and $\omega_n = \frac{n\pi}{b}$.

5.3 Error estimation

To show graphical interpretation of the error estimate discussed in Section 4, the residual (Equation (6)) against the number of harmonics plots for case I and II are shown in Figures 6(a) and 6(b), respectively. It can be seen clearly that in both cases a zeros convergence is obtained as $N \to \infty$.

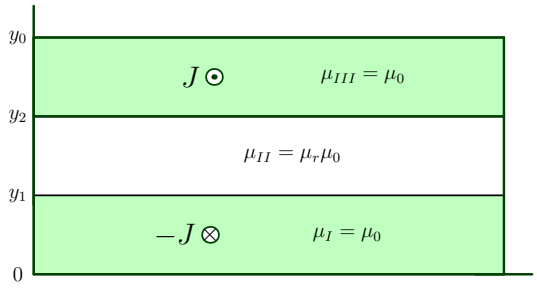

(a)

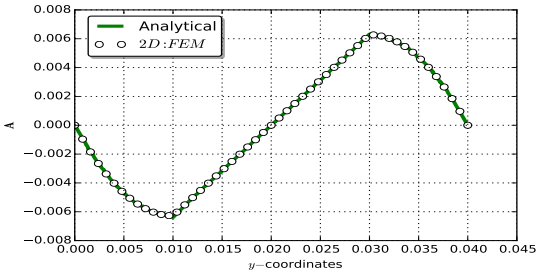

(b)

Figure 5: (a) Material properties; (b) Graphical representations: FEM and Analytical

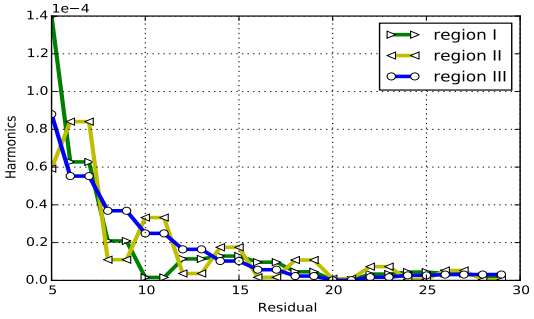

(a)

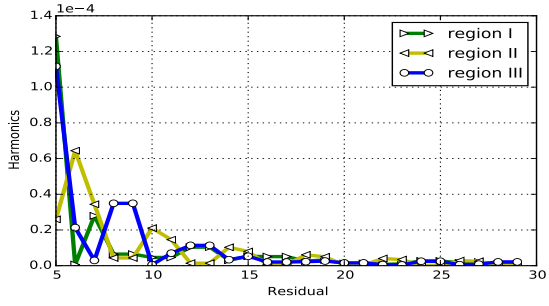

(b)

Figure 6: Convergence plots (a) Case I; (b) Case II

6. CONCLUSION

In this paper a new analytical solution technique has been proposed for magneto-static field problems. The method presented is based on the resolution of the Poisson's equation by using Fourier transform to derive a convergent analytical solution in form of a series. Numerical comparison of the method with the finite element method have shown the method to perform well. The good convergence performance of the method has also been clearly demonstrated. The work presented in this paper has been only implemented for one dimensional magneto-static problems. Future work will extend the application of the method to two-dimensional problems.

7. ACKNOWLEDGEMENTS

This work was supported by Subcommittee B: Postdoctoral fellowship of Stellenbosch University.

REFERENCES

[1] R. Ravaud, G. Lemarquand, V. Lemarquand and C. Depollier, "Analytical calculation of the magnetic field created by permanent-magnet rings", *IEEE Trans. Magn.*, vol. 44, no. 8, pp. 1982-1989, August 2008.

[2] K.J. Strnat, "Modern permanent magnets for applications in electro-technology," in Proceedings of the IEEE, vol. 78, no. 6, pp. 923-946, June 1990.

[3] E.P. Furlani, *Permanent Magnet and Electromechanical Devices: Materials, Analysis, and Applications*, Elsevier Science, 2001.

[4] Ramón Bargallo, *Finite Elements for Electrical Engineering*, Universitat Politècnica de Catalunya, Electrical Engineering Department, 2006.

[5] A. Chama, A.J. Sorgdrager, and R-J Wang, "Analytical synchronization analysis of line-start permanent magnet synchronous motors", *Progress In Electromagnetics Research M, (PIER M)*, vol. 48, pp. 183-193, 2016.

[6] T. Lubin, S. Mezani, and A. Rezzoug, "Analytical computation of the magnetic field distribution in a magnetic gear", *IEEE Trans. Magn.*, vol. 46, no. 7, pp. 2611-2621, July 2010.

[7] B.L.J. Gysen, et. al., "General formulation of the electromagnetic field distribution in machines and devices using Fourier analysis", *IEEE Trans. Magn.*, vol. 46, no. 1, January 2010.

[8] D. Lovrié, "Accuracy of approximate formulas for internal impedance of tubular cylindrical conductors for large parameters", *Progress In Electromagnetics Research M, (PIER M)*, vol. 16, pp. 171-184, 2011.